Journal of Imaging Informatics in Medicine
https://doi.org/10.1007/s10278-024-01172-0

LightGBM is an Effective Predictive Model for Postoperative Complications in Gastric Cancer: A Study Integrating Radiomics with Ensemble Learning

Wenli Wang[1] · Rongrong Sheng[2] · Shumei Liao[2] · Zifeng Wu[1] · Linjun Wang[3] · Cunming Liu[1] · Chun Yang[1] · Riyue Jiang[4]

Received: 4 February 2024 / Revised: 8 May 2024 / Accepted: 9 May 2024

Abstract

Postoperative complications of radical gastrectomy seriously affect postoperative recovery and require accurate risk prediction. Therefore, this study aimed to develop a prediction model specifically tailored to guide perioperative clinical decision-making for postoperative complications in patients with gastric cancer. A retrospective analysis was conducted on patients who underwent radical gastrectomy at the First Affiliated Hospital of Nanjing Medical University between April 2022 and June 2023. A total of 166 patients were enrolled. Patient demographic characteristics, laboratory examination results, and surgical pathological features were recorded. Preoperative abdominal CT scans were used to segment the visceral fat region of the patients through 3Dslicer, a 3D Convolutional Neural Network (3D-CNN) to extract image features and the LASSO regression model was employed for feature selection. Moreover, an ensemble learning strategy was adopted to train the features and predict postoperative complications of gastric cancer. The prediction performance of the LGBM (Light Gradient Boosting Machine), XGB (XGBoost), RF (Random Forest), and GBDT (Gradient Boosting Decision Tree) models was evaluated through fivefold cross-validation. This study successfully constructed a model for predicting early complications following radical gastrectomy based on the optimal algorithm, LGBM. The LGBM model yielded an AUC value of 0.9232 and an accuracy of 87.28% (95% CI, 75.61–98.95%), surpassing the performance of other models. Through ensemble learning and integration of perioperative clinical data and visceral fat radiomics, a predictive LGBM model was established. This model has the potential to facilitate individualized clinical decision-making and the early recovery of patients with gastric cancer post-surgery.

Keywords Radiomics · Ensemble learning · Gastric cancer · Postoperative complication

Introduction

Gastric cancer ranks fifth in global incidence and fourth in mortality, with over 1 million new cases recorded in 2020 [1]. Radical gastrectomy is the primary treatment for gastric cancer; however, the occurrence of postoperative complications remains challenging. Globally, the incidence of postoperative complications in gastric cancer patients ranges from 11.5 to 53.9%, while in China, it is approximately 18.14% [2, 3]. These complications significantly impact the early recovery and long-term outcomes of patients undergoing radical gastrectomy, with higher severity correlating with lower relapse-free survival rates [4, 5]. Thus, the development of an accurate predictive model to identify individuals at a high risk of postoperative complications is crucial for early intervention.

✉ Chun Yang
chunyang@njmu.edu.cn

✉ Riyue Jiang
riyuejiang@jsph.org.cn

1 Department of Anesthesiology and Perioperative Medicine, The First Affiliated Hospital of Nanjing Medical University, Nanjing 210029, China

2 Information Center, The First Affiliated Hospital of Nanjing Medical University, Nanjing 210029, China

3 Department of Gastric Surgery, The First Affiliated Hospital of Nanjing Medical University, Nanjing 210029, China

4 Department of Radiation Oncology, The First Affiliated Hospital of Nanjing Medical University, Nanjing 210029, China

Published online: 28 June 2024

The inflammatory response is an independent risk factor for poor prognosis in patients with cancer. For every one standard deviation increase in inflammatory load, there was a 10.3% increase in the risk of poor prognosis in cancer patients [6]. The dysregulation of the systemic inflammatory response after surgery is closely linked to complications such as incision infection, anastomotic leakage, and cardiopulmonary issues [7, 8]. Inflammatory status significantly affects cancer-related mortality [9]. Obesity is characterized by chronic low-grade systemic inflammation [10], which can contribute to the development of insulin resistance [11]. Adipose tissue secretes numerous pro-inflammatory factors, and over 15 adipocytokines have been linked to cancer [12–14]. In an inflammatory and hypoxic environment, adipocytes release a variety of adipokines, maintain the inflammatory state, promote angiogenesis, and provide energy for tumor cells, thereby promoting the growth, invasion, and metastasis of cancer cells. In addition, the interaction between dysfunctional adipocytes and cancer cells can also lead to inflammatory and fibrotic changes in adipose tissues [15, 16]. High visceral adipose tissue (VAT) is an independent risk factor for postoperative complications in patients undergoing radical gastrectomy [17]. A recent study showed that visceral fat parameters, such as mean attenuation of visceral fat, are important factors in predicting peritoneal metastasis in patients with gastric cancer [18]. This may be related to the secretion of CXC motif chemokine ligand 2 (CXCL2) by visceral adipocytes to induce the invasiveness of gastric cancer cells and promote peritoneal metastasis [19]. Most studies have focused solely on assessing the visceral fat area, with little exploration of other imaging features [20–23]. Inflammatory markers and visceral fat parameters can effectively indicate early signs of postoperative complications. Integrating a patient's clinical data and radiomic data into a prognostic model is expected to enhance its effectiveness.

The medical field has widely embraced technologies such as artificial intelligence, machine learning, and radiomics to make significant progress in assisting clinicians with individualized disease prevention, early diagnosis, and efficacy evaluation [24, 25]. Machine learning technology has shown great potential in image reconstruction, segmentation, identification, and classification, and is an essential technical basis for radiomics. Moreover, with the related algorithms and development platforms of machine learning gradually mature, it has the unique advantage in processing high-dimensional data, which provides great help for the in-depth analysis of medical images [26]. The machine learning model demonstrated a strong predictive performance in assessing the risk of postoperative complications, surpassing the current general-purpose risk prediction model of the American College of Surgeons National Surgical Quality Improvement (ACS-NSQIP) in terms of sensitivity and specificity. In addition, they were able to identify subtle associations that were not detectable by traditional statistical analysis [27]. However, in the field of prediction of postoperative complications of gastric cancer, most studies focus on traditional statistical models and machine learning algorithms. Due to the low complexity of the model, it fails to perform well in dealing with high-dimensional data and possesses poor generalization ability. This prompted us to explore more advanced algorithms. Ensemble learning can improve generalization performance, reduce error rate, and avoid overfitting by integrating multiple learners to better deal with high-dimensional data and obtain better clinical prediction effect [28].

Radical gastrectomy is prone to many postoperative complications, which is an urgent clinical problem that needs to be better solved. Based on the correlation between inflammation, obesity, and postoperative complications and the limitations of current work, this study innovatively integrated the radiomics of visceral fat and clinical inflammation and used four ensemble learning algorithms (LGBM, GBDT, XGB, and RF) to construct a prediction model for postoperative complications of gastric cancer. Through the verification of the prediction performance of the model, the best model is selected to assist clinicians in early warning of potential high-risk groups of complications, timely intervention of possible complications, and ultimately promote early postoperative rehabilitation for patients.

Materials and Methods

Patients

A total of 213 patients who underwent radical gastrectomy for gastric cancer at the First Affiliated Hospital of Nanjing Medical University between April 2022 and June 2023 were retrospectively enrolled. Based on the exclusion criteria, 166 patients were finally included in the analysis (Fig. 1). Ethical approval for this study (Approval No. 2022-SR-591) was provided by the Ethics Committee of the First Affiliated Hospital of Nanjing Medical University, Nanjing, China on 22 November 2022. And the requirement for informed consent was waived.

The inclusion criteria were as follows: (1) age $\geq$ 18 years, (2) clinical diagnosis of primary gastric cancer, (3) radical gastrectomy, (4) preoperative abdominal CT examination within 1 month, and (5) complete perioperative clinical data.

The exclusion criteria were as follows: (1) incomplete or low-quality CT images, inability to delineate the region of interest or data analysis, (2) infection within 2 weeks before surgery, and (3) preoperative complications such as bleeding, obstruction, perforation, or distant metastasis.

Baseline data, laboratory examination results, and early postoperative complications were collected. The baseline

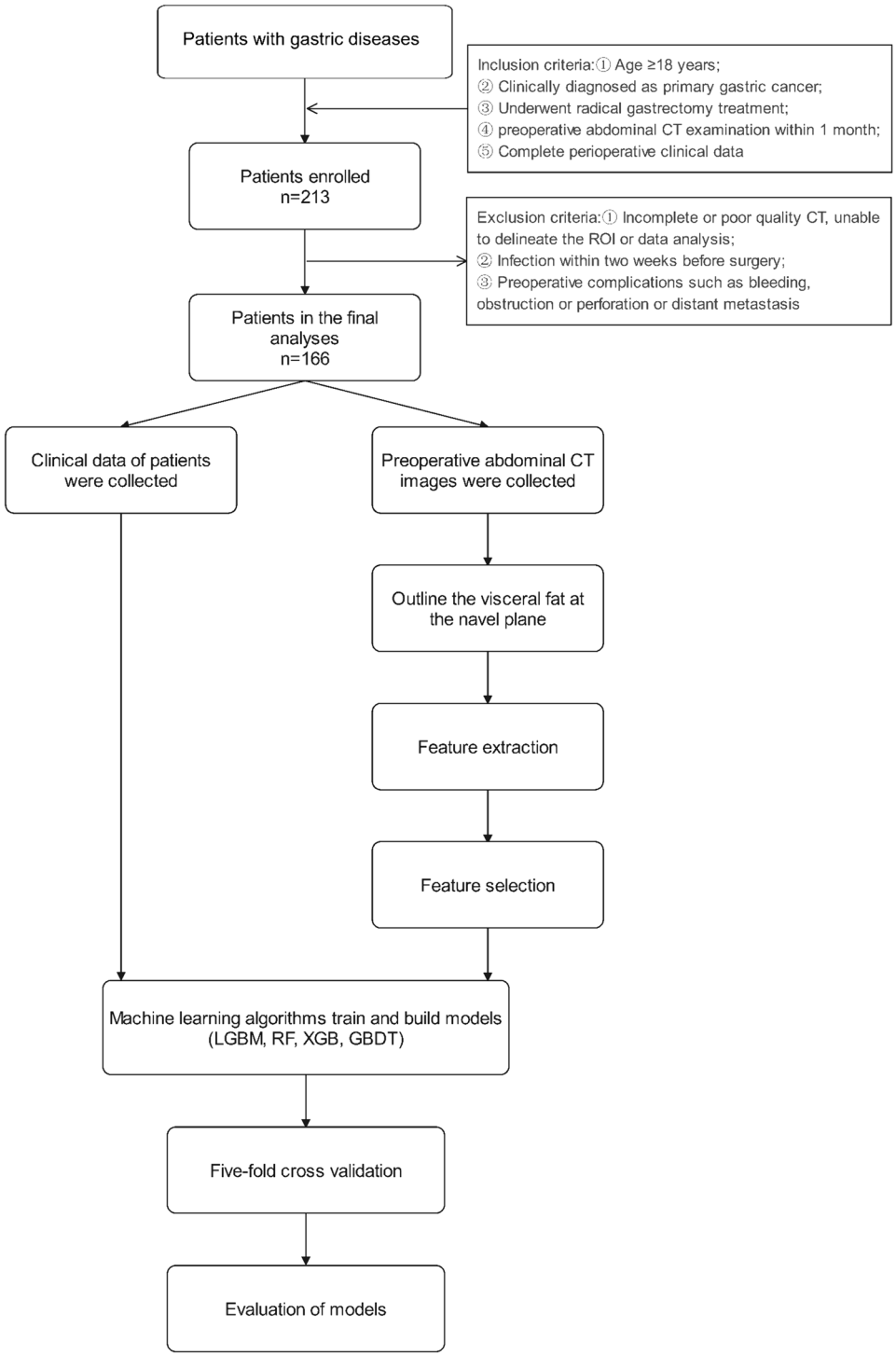

Fig. 1 Flow chart

data included many factors such as sex, age, BMI, smoking history, comorbidities, TNM stage, chemotherapy history, Borrmann classification, and Lauren classification. In addition, a series of laboratory indicators were included, such as CA125, CA153, CA724, AFP, CEA, and CA199, as well as the preoperative and postoperative neutrophil count, lymphocyte count, monocyte count, and albumin level. To assess inflammation and immune response more accurately, we calculated the preoperative and postoperative lymphocyte-to-monocyte ratio (LMR), platelet-to-lymphocyte ratio (PLR), neutrophil-to-lymphocyte ratio (NLR), and systemic immunoinflammatory index (SII). SII is defined as the platelet count × neutrophil count/lymphocyte count.

Preoperative abdominal enhanced CT was collected, and the CT parameters were as follows: kV, 120 kV; mA mode, SmartmA 400–700; scan type, helical; rotation time, 0.50 s; detector coverage, 80 mm; contrast agent, ioversol injection, 100 mL; image matrix, 512×512; reconstruction image thickness, 5 mm.

According to the "Chinese Expert Consensus on the Diagnosis and Registration of Postoperative Complications of Gastrointestinal Cancer Surgery," complications occurred within 30 days after surgery were counted, including the following eight categories: gastrointestinal complications, surgical site complications, respiratory complications, cardiovascular complications, thromboembolic complications, urinary complications, infectious complications, and other complications. Among them, gastrointestinal complications include anastomotic leakage, abdominal/pelvic infection, pancreatic fistula, hemorrhage, intestinal obstruction, and delayed gastric emptying. Surgical site complications include wound dehiscence, infection, fat liquefaction, and delayed wound healing. Respiratory complications included postoperative atelectasis, pneumonia, pleural effusion, and empyema. Cardiovascular complications refer to postoperative arrhythmia, heart failure, myocardial infarction, etc.

Data Pre-processing

CT Data Cleaning and Optimization

In our study, the quality and accuracy of CT data are of utmost importance, directly influencing subsequent image processing and analysis outcomes [29]. We initiated a series of cleaning and optimization processes on the raw CT images to ensure data quality and accurate analysis. First, we employed advanced denoising algorithms to identify and eliminate noise and disturbances in the images, thus enhancing the image clarity and precision in detail. Based on denoising, we applied filtering techniques to further optimize the image quality by eliminating both low- and high-frequency interferences, preserving the main features and details of the images. During the cleaning process of CT data, specific methods for noise filtering and outlier removal of the data include the use of Gaussian filters and anomaly detection based on Z scores [30, 31].

Subsequently, we adjusted the contrast of the images to highlight the details, facilitating subsequent feature extraction and analysis. We adopted adaptive contrast adjustment techniques that dynamically alter the contrast levels based on the specific content and characteristics of the image. It emphasizes different areas and details, which improves the overall image quality and analyzability.

Data Augmentation

Owing to the specificity and complexity of gastric cancer imagery, there could be significant imbalances in the distribution of samples from different categories and types. This could lead the model to learn and predict biases towards certain specific categories or features, thereby affecting its overall predictive performance and accuracy. To enhance the generalization capabilities and predictive accuracy of the model, we utilized data augmentation techniques to expand and optimize the original data. In the data enhancement stage, we applied three techniques including random rotation ($\pm 30°$), scaling (0.8 to 1.2 times), and horizontal flipping to improve the model's adaptability to different viewing angles and scales. Thus, the image features can be better presented and the learning and recognition ability of the model can be improved.

Through the integrated use of the above data cleaning and augmentation techniques, the quality and diversity of the CT image data were ensured, which laid a solid foundation for subsequent feature extraction, model training, and complication prediction.

Region of Interest (ROI) Segmentation

The segmentation of the region of interest (ROI) referred to in this study focused on visceral fat within the umbilical horizontal plane. A trained diagnostic imaging specialist independently conducted the segmentation. The initial range of CT values (-150,-50) Hu was established within the umbilical plane. Subsequently, the 3D Slicer software (version 5.0.3) was utilized to semi-automatically segment the visceral fat area during the portal vein stage of the abdominal enhanced CT scan. This process aimed to obtain an approximate area of the visceral fat tissue. Following the semi-automatic segmentation, manual boundary adjustments were made to ensure a more precise delineation of the visceral fat tissue.

Feature Extraction and Selection

3D-CNN Feature Extraction

We employed a 3D-CNN (Three-Dimensional Convolutional Neural Network) to extract radiomic features of the adipose region from CT images of patients with gastric cancer. Specifically, using the PyTorch framework, we implemented a 3D-CNN model composed of multiple convolutional and pooling layers. The model's architecture is as follows. Initially, the input layer accepts single-channel three-dimensional image data. This is followed by the first convolutional layer (with 32 $3 \times 3 \times 3$ kernels, stride of 1, and padding of 1) and

a ReLU activation function for feature extraction and nonlinear mapping. Subsequently, a max-pooling layer (with $2 \times 2 \times 2$ pooling kernels)is used for downsampling. The second convolutional layer contained 64 $3 \times 3 \times 3$ kernels with stride and padding unchanged and then passed through ReLU activation and max-pooling. The third convolutional layer employs 128 $3 \times 3 \times 3$ kernels, which are consistent with the parameters of the preceding layers, followed by a global average pooling layer for feature aggregation. Finally, a $1 \times 1 \times 1$ convolutional layer reduced the feature dimensionality to 300 dimensions. This design ensures rich and representative features from intricate three-dimensional CT images, thereby setting the stage for subsequent feature selection and model training.

Key Radiomic Feature Selection

After the 3D-CNN feature extraction, we obtained a 300-dimensional feature vector for each sample. To enhance the interpretability and predictive performance of a model, it is essential to further refine these features and retain only the most informative and representative features. We used the LASSO regression model for feature selection. By introducing an L1 regularization term into the regression model's objective function, LASSO can automatically select features, compressing the weights of less relevant features to zero [32].

By adjusting the regularization strength α of the LASSO model, we controlled the model's complexity and the strictness of feature selection. Within a cross-validation framework, we identified the optimal α value that delivered the best predictive performance and determined the final set of features. These features not only offer a sound interpretation of the underlying mechanisms of postoperative complications in gastric cancer but also provide robust feature support for our predictive model, aiding in a more precise prognosis of postoperative complication risks for gastric cancer patients.

Construction of the Prediction Model

Early machine learning models, such as single decision trees and rudimentary neural networks, were often limited by their generalization capabilities. These models are often prone to overfitting in the face of complex data distributions and are very sensitive to noise and outliers. Furthermore, they do not work well when dealing with high-dimensional data because the simplicity of the models limits their ability to capture complex patterns. To overcome the limitations of the earlier models, we introduced an ensemble learning strategy. In this study, we used the Light Gradient Boosting Machine (LGBM), XGBoost (XGB), Random Forest (RF), and Gradient Boosting Decision Tree (GBDT) models for feature learning and complication prediction. The LGBM employs a histogram-based decision tree algorithm, which effectively handles large-scale data while maintaining high accuracy. XGB is an extensible and flexible gradient-boosting algorithm with features such as the automatic handling of missing values and regularization to reduce overfitting. RF utilizes multiple decision trees for training and enhances prediction accuracy and robustness through a voting mechanism. The GBDT constructs multiple decision trees in a stepwise optimization manner, with each tree learning the residuals of the previous tree, continuously improving the model's predictive performance. In this study, we combined selected radiomic features with preoperative and postoperative clinical features and input them into each model for training (Fig. 2).

Regarding the training details and specific parameter settings for each model, in the LGBM model, we set the learning rate to 0.01 and the number of trees to 100 to ensure learning precision and generalization ability. We also apply feature and data subset sampling to enhance the robustness of the model. For XGBoost, we selected a learning rate of 0.1 and a tree depth of 6 to balance learning efficiency and accuracy, and pruning was enabled to prevent overfitting. In the RF model, we configured 100 trees and determined the maximum feature count automatically to achieve high accuracy. The settings for GBDT included a learning rate of 0.05 and 50 trees to ensure model learning and predictive performance. All model parameters were optimized through cross-validation and a grid search to achieve the best performance in predicting complications after gastric cancer surgery.

Our ensemble learning model fully considers the strengths of each base model and combines their predictive abilities to achieve higher accuracy and robustness. By employing multiple models, this strategy mitigated the challenges posed by data heterogeneity and complexity for a single model, thereby enhancing the adaptability and predictive capabilities of the model for different gastric cancer cases and types of complications.

Model Evaluation

In the model evaluation phase, we used accuracy (Acc), recall, precision, F1-score, and area under the receiver operating characteristic curve (AUC-ROC) as evaluation metrics. Accuracy represents the proportion of correctly predicted samples to the total number of samples and is used to measure the overall performance of the model. Recall focuses on the proportion of true positive samples correctly identified by the model among all actual positive samples, emphasizing the model's ability to recognize positive samples. Precision focuses on the proportion of correctly identified positive samples among the samples predicted as positive,

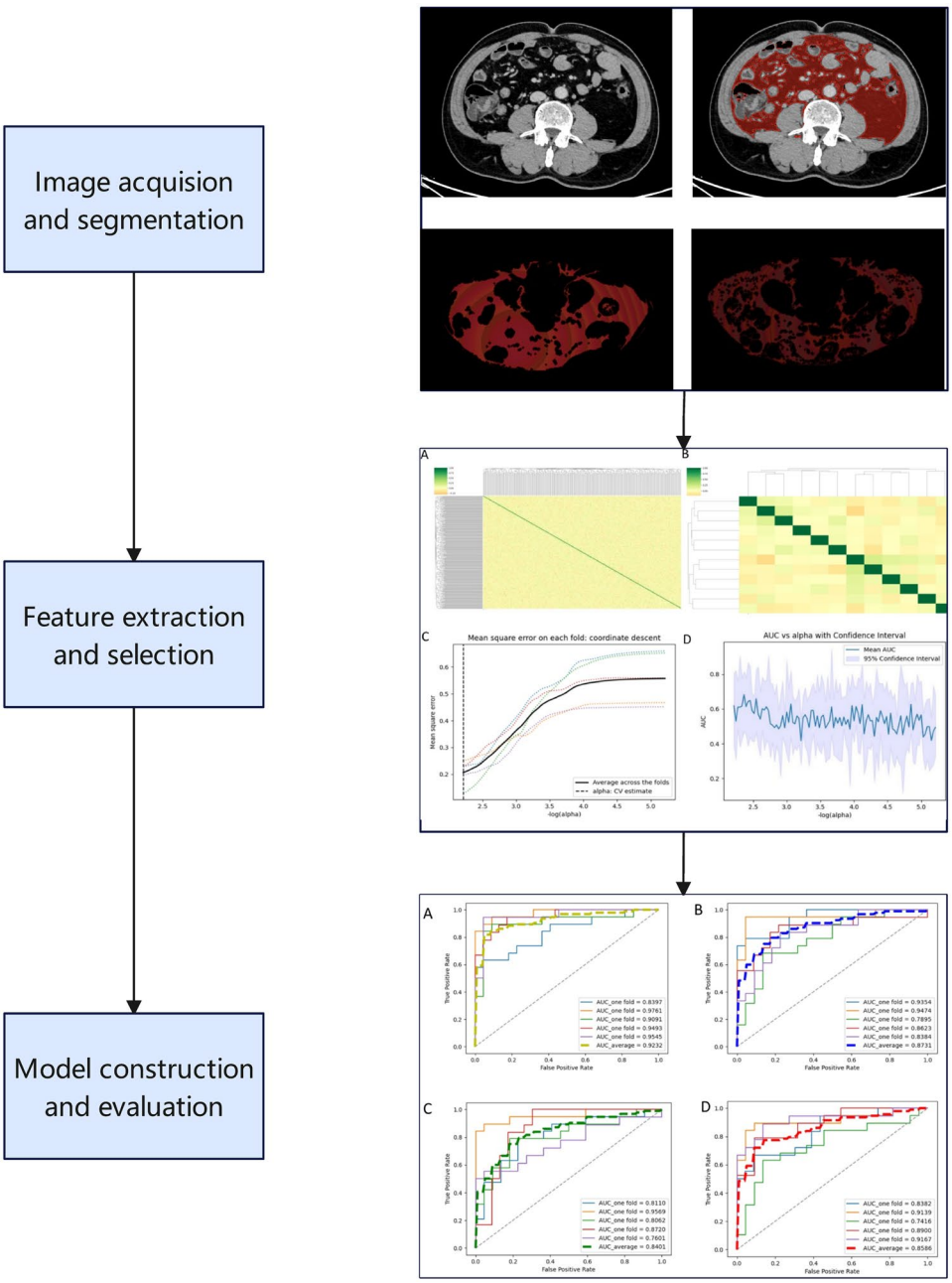

Fig. 2 Summary diagram of main research contents The main research contents include image acquisition and segmentation, feature extraction and selection, and model construction and evaluation

evaluating the prediction accuracy [33]. The F1-score is the harmonic mean of the precision and recall, providing a comprehensive assessment of the robustness [34]. The AUC-ROC reflects the overall performance of the model in classifying positive and negative samples; a higher value indicates better classification performance [35]. For result representation, we calculated the average evaluation metric values from cross-validation experiments and computed their 95% confidence intervals (CI). We comprehensively assessed the performance of all models using these evaluation metrics to ensure their accuracy and reliability in predicting complications after gastric cancer surgery.

Results

Experimental Setup

In this study, we employed fivefold cross-validation to evaluate the performance of all models. During this process, all data were randomly divided into five subsets, with four subsets used as training data every time, and the remaining one subset was used as the test data. This process was repeated five times with different test sets each time to obtain performance metrics for the models on different data subsets. Each model was trained and tested on the same data partitions

Table 1 Baseline information of clinical characteristics in gastric cancer patients

Value	Total ($n = 166$)	Postoperative complications		*P* value
		No ($n = 122$)	Yes ($n = 44$)	
Sex, *n* (%)				0.779
Men	118 (71.08)	86 (70.49)	32 (72.73)	
Women	48 (28.92)	36 (29.51)	12 (27.27)	
Age (years)	65.00 (57.00–70.00)	66.00 (57.00–70.00)	62.00 (56.75–70.00)	0.750
BMI (kg/m^2, mean ± SD)	24.24 ± 2.91	24.18 ± 3.00	24.40 ± 2.65	0.668
Operation method, *n* (%)				0.102
Open	19 (11.45)	11 (9.02)	8 (18.18)	
Laparoscope	147 (88.55)	111 (90.98)	36 (81.82)	
Chemotherapy, *n* (%)				0.618
No	152 (91.57)	113 (92.62)	39 (88.64)	
Yes	14 (8.43)	9 (7.38)	5 (11.36)	
Smoking, *n* (%)				0.622
No	112 (67.47)	81 (66.39)	31 (70.45)	
Yes	54 (32.53)	41 (33.61)	13 (29.55)	
Comorbidities, *n* (%)				0.128
No	88 (53.01)	69 (56.56)	19 (43.18)	
Yes	78 (46.99)	53 (43.44)	25 (56.82)	
TNM stage, *n* (%)				0.261
I	54 (32.53)	42 (34.43)	12 (27.27)	
II	18 (10.84)	14 (11.48)	4 (9.09)	
III	22 (13.25)	14 (11.48)	8 (18.18)	
IV	65 (39.16)	49 (40.16)	16 (36.36)	
V	7 (4.22)	3 (2.46)	4 (9.09)	
Borrmann classification, *n* (%)				0.505
I	30 (18.07)	21 (17.21)	9 (20.45)	
II	46 (27.71)	35 (28.69)	11 (25.00)	
III	78 (46.99)	57 (46.72)	21 (47.73)	
IV	12 (7.23)	9 (7.38)	3 (6.82)	
Lauren classification, *n* (%)				0.824
Enteric	73 (47.1)	54 (46.96)	19 (47.50)	
Diffuse	36 (23.23)	28 (24.35)	8 (20.00)	
Mixed	57 (34.34)	40 (32.79)	17 (38.64)	
CA125 (U/ml)	9.40 (7.00–13.88)	9.60 (6.85–14.00)	9.40 (7.35–13.35)	0.973
CA153 (U/ml)	8.26 (6.34–11.49)	8.21 (6.32–11.62)	8.26 (6.65–10.07)	0.646
CA724 (μg/L)	1.91 (1.23–3.42)	1.97 (1.19–3.54)	1.67 (1.28–2.83)	0.665
AFP (ng/mL)	2.43 (1.69–3.11)	2.37 (1.65–3.08)	2.58 (1.94–3.12)	0.286
CEA (ng/mL)	2.33 (1.56–3.75)	2.31 (1.57–3.71)	2.38 (1.55–3.74)	0.996
CA199 (u/ml)	9.06 (4.96–19.80)	10.06 (5.00–20.04)	8.80 (4.66–14.83)	0.487
Preoperative albumin (g/L)	38.50 (35.73–40.27)	38.45 (35.73–40.30)	38.80 (35.65–40.12)	0.910
Postoperative albumin, (g/L, mean ± SD)	35.53 ± 3.77	36.12 ± 3.56	33.89 ± 3.91	$< .001^{***}$
Albumin change value (g/L)	-3.15 (-5.80–0.08)	-2.15 (-5.40–0.80)	-4.50 (-6.92 to-2.40)	0.006^{**}
Preoperative inflammatory markers				
Neutrophil(10^9/L)	2.95 (2.24–3.71)	2.94 (2.22–3.55)	3.08 (2.32–3.92)	0.477
Lymphocyte(10^9/L)	1.46 (1.17–1.89)	1.46 (1.14–1.87)	1.46 (1.20–1.94)	0.749
Monocyte(10^9/L)	0.42 (0.34–0.53)	0.42 (0.33–0.52)	0.47 (0.36–0.56)	0.189
NLR	1.96 (1.45–2.73)	1.97 (1.45–2.66)	1.96 (1.55–2.79)	0.606
LMR	3.49 (2.68–4.58)	3.58 (2.71–4.66)	3.41 (2.51–4.42)	0.295
PLR	138.06 (105.80–174.42)	135.33 (103.28–184.57)	143.32 (113.50–168.26)	0.612

Table 1 (continued)

Value	Total ($n=166$)	Postoperative complications		*P* value
		No ($n=122$)	Yes ($n=44$)	
SII	402.00 (255.77–585.46)	389.08 (252.69–585.46)	468.75 (278.58–583.27)	0.379
Postoperative inflammatory markers				
Neutrophil(10^9/L)	9.96 ± 3.07	9.50 ± 3.02	11.24 ± 2.86	0.001***
Lymphocyte(10^9/L)	0.84 (0.63–1.16)	0.85 (0.60–1.16)	0.82 (0.68–1.09)	0.842
Monocyte(10^9/L)	0.66 ± 0.37	0.61 ± 0.36	0.80 ± 0.36	0.002**
NLR	11.68 (8.47–15.44)	11.41 (8.02–15.09)	13.58 (9.57–16.75)	0.074
LMR	1.33 (1.00–2.25)	1.41 (1.07–2.50)	1.09 (0.82–1.51)	0.001***
PLR	215.82 (150.18–306.72)	204.40 (142.69–306.06)	246.51 (177.13–312.49)	0.193
SII	2033.84 (1421.59–3179.52)	1917.28 (1351.70–3017.24)	2523.68 (1778.93–3876.01)	0.013*

Normally distributed data were analyzed using independent *t*-tests, and the results are presented as mean ± standard deviation. Non-normally distributed data were analyzed using the Mann–Whitney U test, and the results are presented as medians and interquartile ranges. Categorical variables are analyzed using chi-square tests, and the results are expressed as percentages. The asterisk (*) indicates that these measures are statistically different between patients without complications and those with complications. The asterisk (*) represents P value ≤ 0.05; the asterisk (**) represents P value ≤ 0.01; the asterisk (***) represents P value ≤ 0.001. The results in this table demonstrate that postoperative values of neutrophils, monocytes, LMR, SII, albumin, and perioperative albumin were significantly different between the two groups. *BMI* body mass index, *Mean* average, *SD* standard deviation, *NLR* neutrophil-to-lymphocyte ratio, *LMR* lymphocyte-to-monocyte ratio, *PLR* platelet-to-lymphocyte ratio, *SII* systemic immunoinflammatory index

to ensure consistency and fairness during the evaluation. Furthermore, we conducted extensive hyperparameter tuning through detailed grid search and random search to optimize the parameters for each model. We monitored the training and validation losses for each model, confirming that all models converged and showed no signs of significant overfitting. The experiments were conducted on a high-performance computer equipped with an NVIDIA RTX 3070 GPU and Intel RYZEN7 CPU. Python was used as the primary program language, and open-source libraries such as Scikit-learn, LightGBM, and XGBoost were used for model implementation and optimization. The operating system used was Ubuntu 20.04 LTS, ensuring stability and efficiency in the software and hardware environment.

Statistical Analysis of Basic Clinical Information for Patients

To investigate the relationship between patient complications and baseline clinical data, we conducted a detailed statistical analysis of the clinical information for every patient. An independent *t*-test was used to analyze normally distributed data, the Mann–Whitney U test was used to analyze non-normally distributed data, and the chi-square test was used to analyze categorical variables. We integrated all data into a "Statistical Table of Patient Basic Information" (Table 1).

One hundred and sixty-six patients (118 males and 48 females) were enrolled in this study. Significant differences were identified by comparing patients who experienced complications with those who did not experience complications. Statistical analysis demonstrated that the *P* values for postoperative neutrophils, monocytes, LMR, SII, albumin, and perioperative albumin were all < 0.05. This suggests that these characteristics are associated with the occurrence of complications.

In the short-term postoperative outcomes, 44 patients had postoperative complications (Table 2). Interestingly, among all postoperative complications, we found that postoperative pulmonary complications had the highest probability, with a total of 24 cases.

Table 2 Postoperative complications

Postoperative complications	Number
Fever	1
Lymphatic fistula	1
Anastomotic leak	4
Pulmonary complications*	24
Incision infection	4
Incision fat liquefaction	2
Abdominal infection	3
Abdominal hemorrhage	1
Stump fistula	1
Elevated aminotransferase	2
Gastrointestinal dysfunction*	5

If patients had two or more postoperative complications, we repeated the count. Pulmonary complications* include pulmonary infection, atelectasis, empyema, and pulmonary embolism. Gastrointestinal dysfunction* including postoperative nausea and vomiting and intestinal obstruction

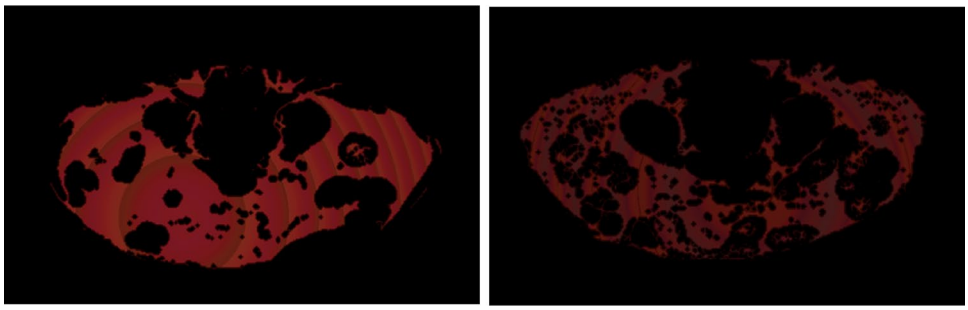

Fig. 3 Segmentation of visceral fat regions of interest based on CT images. Among them, the left is the visceral fat of patients without complications, and the right is the visceral fat of patients with complications

Results of Feature Extraction and Selection

In the process of patient feature extraction based on 3DCNN, 300-dimensional feature information was successfully extracted from expert-annotated fat regions (Fig. 3), providing a rich dataset for subsequent analysis. However, in order to construct an efficient and accurate prediction model, it is essential to simplify the feature space and eliminate redundant features. Thus, a feature selection process using the LASSO regression method was conducted, ultimately leading to the selection of 12 key radiomic features for application in subsequent models.

To illustrate the feature selection process and its effectiveness visually, a series of visualizations were employed. The correlation heatmaps before and after feature selection are presented in Fig. 4a and b, respectively. These heatmaps demonstrated a notable decrease in feature correlations following selection, indicating the elimination of highly correlated features and the provision of unique information to the model by each feature. Additionally, Fig. 4c shows the relationship between the penalty term coefficient (α) and the mean squared error throughout the iterations of the LASSO model. Furthermore, Fig. 4d shows the variation in AUC with changes in the penalty term coefficient. Through a

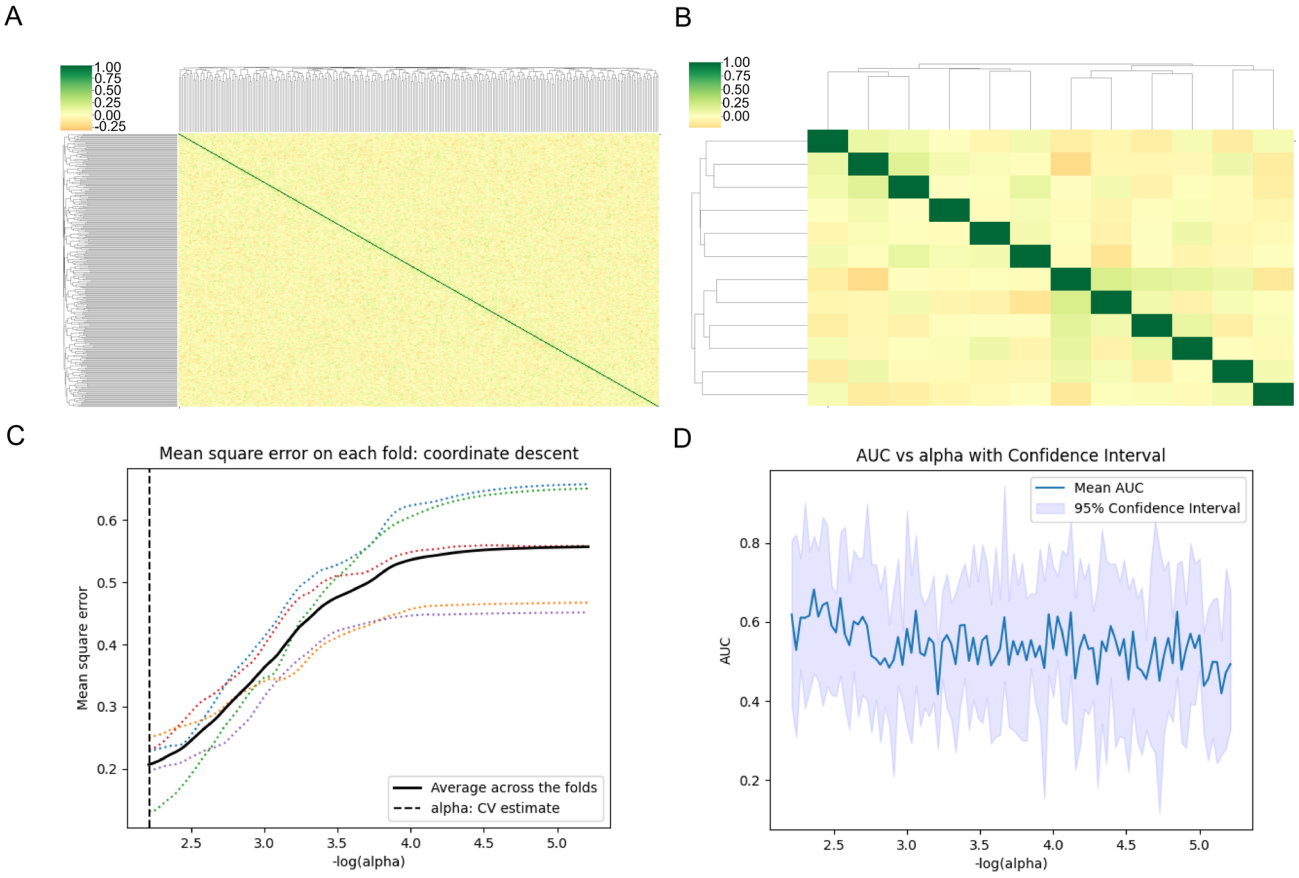

Fig. 4 Visual results of the feature selection process. Correlation heatmaps before and after feature selection (**A**, **B**). The process of feature selection model iterations (**C**), and the selection results for different feature dimensions (**D**)

thorough examination of the iterative results, α was identified as the optimal parameter for the LASSO regression, with a value of 0.004. This parameter selection resulted in a stable model and a satisfactory predictive performance.

Complication Prediction Model Results

Training Process

Throughout the training process of our complication prediction model, we incorporated a diverse range of advanced techniques and strategies to enhance efficiency and guarantee stability. To leverage the benefits of automatic learning rate adjustment and accommodate varying data characteristics, we opted for Adam as the optimizer, a choice backed by its exceptional performance across various tasks. To expedite convergence to the optimal solution in the initial stages of training and avoid being ensnared in suboptimal local solutions, we tailored the initial learning rates for each model based on specific circumstances. Moreover, to strike a balance between model stability and memory utilization, we carefully deliberated the choice of a batch size of 32, considering the dataset size and available computational resources.

Light GBM Ensemble Learning Model Results

We adopted the ensemble learning LGBM model, which demonstrated remarkable performance across various evaluation metrics. Notably, the model achieved an impressive ROC-AUC value of 0.9232, indicating an exceptional predictive capability. Furthermore, the high levels of recall and precision attained by the model provided additional evidence of its robustness and reliability. The visualization of the ROC curve in Fig. 5a clearly indicates the excellent discriminative power of the model between the positive and negative classes. This observation was corroborated by the cross-validation comparison in Table 3.

Results of Other Ensemble Learning Models

We compared our adopted LGBM model with other commonly used ensemble learning models, such as RF, GBDT,

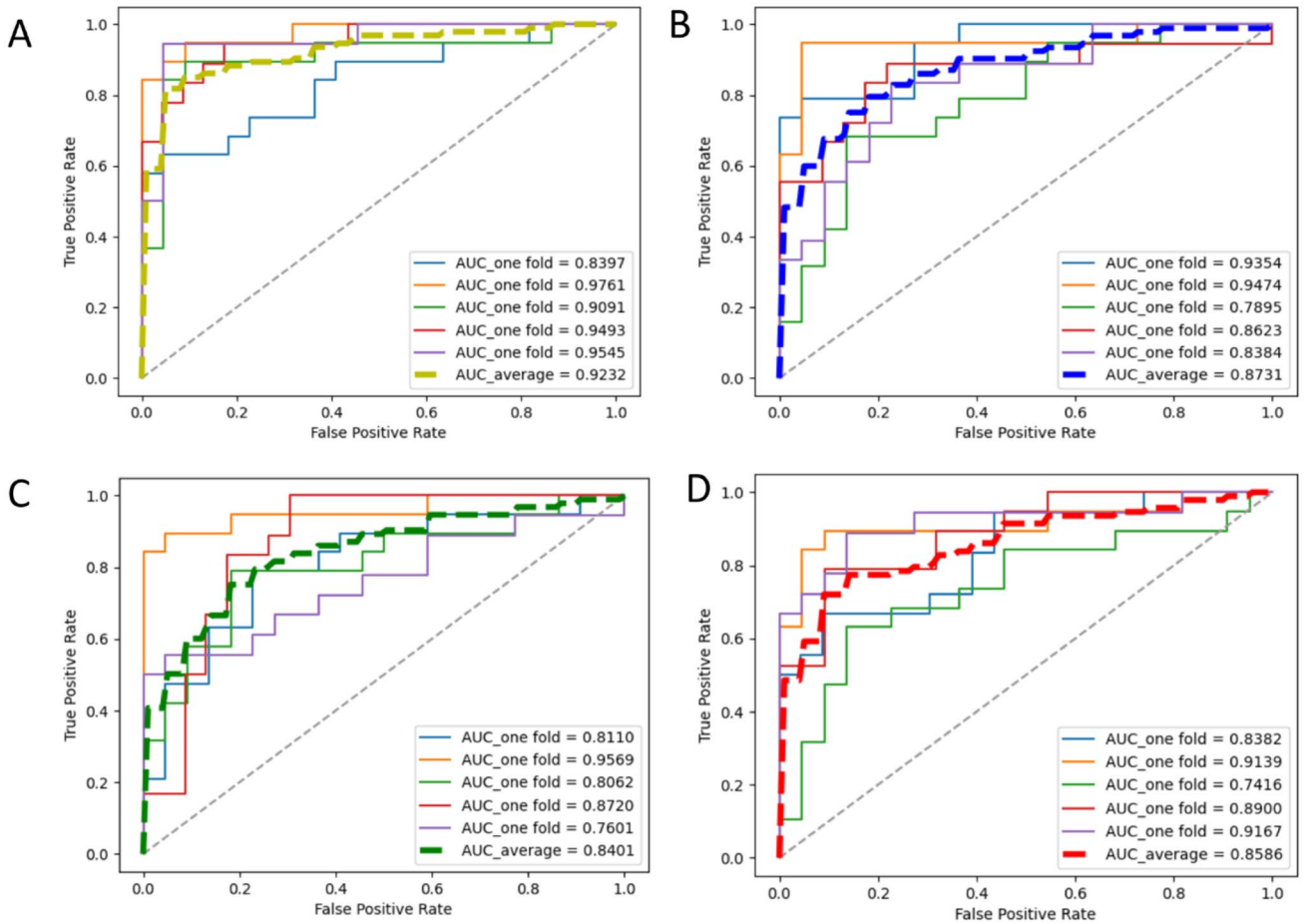

Fig. 5 ROC curves and AUC values for various prediction models where **A**, **B**, **C**, and **D** represent LGBM, RF, GBDT, and XGB, respectively. As can be seen from the figure, the LGBM model has the highest AUC value, and the prediction efficiency is better than other models

Table 3 Performance of various models in five-fold cross-validation

Model	Acc	Recall	Prec	F1
LGBM	87.28% (75.61–98.95%)	81.81% (63.16–100.46%)	89.11% (80.00–98.22%)	85.14% (70.59–99.69%)
RF	84.29% (78.05–90.53%)	79.54% (68.42–90.66%)	85.14% (75.00–95.28%)	82.03% (74.29–89.77%)
GBDT	78.47% (70.00–86.94%)	76.14% (55.56–96.72%)	78.02% (69.57–86.47%)	75.41% (62.50–88.32%)
XGB	77.99% (68.29–87.69%)	71.00% (55.56–86.44%)	80.97% (65.00–96.94%)	74.43% (62.50–86.36%)

The accuracy, recall, precision, and F1 score of the LGBM, RF, GBDT, and XGB models in fivefold cross-validation. The performance of each model is presented as the mean value along with its 95% confidence interval (CI)

and XGB. Although these models exhibited a good performance on most evaluation metrics, they ultimately fell short of the LGBM model. For example, RF achieved an ROC-AUC value of 0.8731, and XGB scored 0.8586, both of which were lower than the performance of the LGBM model. The ROC curves demonstrated the relatively weaker ability of these models to distinguish between positive and negative samples (Fig. 5b–d). Additionally, the cross-validation comparison in Table 3 offers detailed performance on various evaluation metrics, further confirming the superiority of the LGBM model over other models.

Discussion

We successfully developed the LGBM model capable of predicting early postoperative complications in patients with gastric cancer. This is an efficient machine learning algorithm based on the gradient boosting framework. We use the grid search technique to optimize the main parameters such as the learning rate, the number of trees, and the maximum depth of trees, and finally select the best combination of parameters to achieve the best classification effect. The AUC value in the LGBM model reached 0.92, indicating a high level of accuracy and prediction efficiency, which is significantly superior to that of the GBDT, RF, and XGB models. This model is based on easily obtainable clinical data, laboratory measurements, and CT examination images, making it suitable for widespread application in clinical practice. It can assist in identifying high-risk groups for postoperative complications of gastric cancer, enabling timely adjustments to clinical decision-making and proactive interventions.

After surgical trauma, a protective inflammatory response is mobilized as part of the innate immune system, contributing to the healing of the surgical incision and serving as a natural defense mechanism. However, when the systemic inflammatory response becomes dysregulated, with an abnormal duration and extent, it transitions from a protective response to exacerbating the cycle of tissue damage and immunosuppression. This imbalanced immunoinflammatory response frequently contributes to elevated postoperative complications and mortality, heightening susceptibility to postoperative infections, accelerating tumor recurrence, and prompting the onset of multiple organ dysfunction [36, 37]. Previous studies have demonstrated that the lymphocyte-to-monocyte ratio (LMR) serves as an effective surrogate marker for the proportion of tumor-infiltrating lymphocytes and tumor-associated macrophages. These two types of immune cells play crucial roles in regulating cellular and humoral immunity, as well as in mounting an anti-tumor response. Furthermore, they are also associated with immunosuppression, which can accelerate tumor progression [38]. Kim et al. demonstrated that a low LMR is an independent prognostic factor for gastric cancer patients and is associated with higher postoperative mortality and poorer long-term survival [39, 40]. The neutrophil-to-lymphocyte ratio (NLR) serves as a predictor of postoperative complications in gastric cancer patients. An NLR value of ≥ 9.6 on the second day after surgery indicates a higher risk of postoperative complications [41]. Patients with gastric cancer display high levels of inflammatory factors such as interleukin-6 (IL-6) and tumor necrosis factor-α (TNF-α), which are significant predictors of postoperative outcomes. Notably, elevated levels of these inflammatory cytokines have been linked to poorer 5-year survival rates in gastric cancer, and IL-6 has been established as an independent risk factor for postoperative infection. Hence, the presence of IL-6 and TNF-α in patients with gastric cancer may serve as indicators of poor prognosis and a higher susceptibility to postoperative complications [42]. High levels of matrix metalloproteinase (MMP) - 3,- 7,- 9,- 11, and the increased expression of chemokine receptors CCR- 3,- 4,- 5,- 7, and CXCR-4 are closely associated with poor prognosis in gastric cancer patients [43]. Routine measurement of cytokines in clinical practice is expensive and difficult to perform. Conversely, the use of indicators such as LMR and NLR offers a simple, fast, convenient, and cost-effective method for evaluating the systemic inflammatory immune status in predicting the

prognosis of patients with gastric cancer. This approach provides a viable alternative for costly and operationally challenging routine cytokine measurements, making it a practical option for clinical applications.

Obesity is a well-established risk factor for postoperative complications and a poor prognosis following digestive tract surgery. Obesity significantly increases the likelihood of several adverse outcomes, including postoperative incision infection, anastomotic leakage, intestinal obstruction, and cardiopulmonary complications. Moreover, obesity has been shown to adversely affect the efficacy of chemotherapy and is associated with decreased survival rates [44]. The traditional approach for assessing obesity relies on body mass index (BMI), which considers an individual's height and weight. However, owing to the significant influence of bone and muscle mass on BMI, it is not entirely accurate for determining the level of obesity and fat. This limitation leads to differing clinical outcomes among individuals with the same BMI, which is attributed to variations in muscle and fat proportions. Consequently, the relationship between BMI and postoperative complications in patients with gastric cancer has resulted in conflicting findings within studies [39, 45]. The development of imaging has made it a more accurate and reliable method for evaluating body composition using CT images to measure visceral fat, subcutaneous fat, and skeletal muscle content [46]. Visceral fat accumulation is more likely to cause metabolic and endocrine dysfunction than subcutaneous fat. This can hinder the exposure of the surgical visual field and identification of organ tissues during surgery, resulting in an increased risk of complications such as surgical site infection, pneumonia, and postoperative pancreatic fistula >[47, 48]. Okada et al. demonstrated that as the visceral fat area increased by 10 cm^2, the incidence of complications after radical gastrectomy also increased by 9% [49]. Prof. Guang Ning's group from Shanghai made a significant contribution by identifying the texture characteristics of visceral fat through imaging omics extraction and machine learning [50]. This novel approach has brought attention to the characteristics of adipose tissue, which are often ignored in most studies predicting the clinical outcome of gastric cancer patients after surgery. These characteristics include pathological changes, immune cell infiltration, angiogenesis, and fibrosis. These findings hold considerable significance in evaluating metabolic disorders and predicting the effect of weight loss after surgery, providing a more comprehensive understanding of the factors influencing patient outcomes [50]. We developed a prediction model for postoperative complications of gastric cancer by extracting numerous characteristic parameters of visceral fat using radiomics, along with inflammation and nutritional indices. This is the first time that such a large number of parameters have been extracted for this purpose.

Most early studies focused on traditional statistical models and machine learning algorithms in the field of predicting postoperative complications of gastric cancer. While these approaches have been successful to some extent, there are obvious limitations, including model complexity, reliance on feature engineering, and inadequate generalization capabilities [51–53]. One major drawback of traditional models is their tendency to emphasize single-model architectures and algorithms, lacking the necessary flexibility and adaptability to address the complex and variable clinical problems associated with post-gastric cancer surgery complications. For instance, SVM may perform poorly when handling nonlinear and high-dimensional data and can be sensitive to parameters and feature selection. These limitations motivated us to explore more advanced and flexible models and algorithms to enhance the accuracy and reliability of predicting complications after gastric cancer surgery.

In this study, we utilized ensemble learning techniques, particularly the LightGBM model within the Boosting algorithm, to anticipate postoperative complications in patients with gastric cancer. The core of Boosting lies in its capacity to amalgamate numerous weak prediction models, namely decision trees, into a potent integrated predictor, progressively rectifying errors in preceding models to boost overall prediction accuracy. Notably, LightGBM exhibited its superiority as an efficient Boosting implementation in our application. Its proficiency in handling large datasets and ability to address unbalanced data, particularly crucial in medical imaging data, was evident. Additionally, LightGBM offers a high level of flexibility and scalability, enabling us to tailor our models to suit specific predictive tasks. Our strategy, merging the intricacies of image-omics features with LightGBM's efficient learning ability, yielded impressive results in predicting postoperative complications in gastric cancer patients, underscoring the potential of employing advanced machine learning techniques in medical image analysis.

Subtle changes in single or multiple inflammatory markers and visceral fat without peritoneal metastasis are often overlooked by clinicians. Based on easily accessible perioperative laboratory tests and preoperative abdominal CT, this study constructed an efficient prediction model for postoperative complications of gastric cancer. Clinicians can make individualized risk prediction according to the situation of different patients, as well as timely and targeted intervention for high-risk populations. In addition, this study innovatively used the radiomics of visceral fat to predict postoperative complications of gastric cancer, which is expected to further explore the specific factors and mechanisms of visceral fat affecting postoperative complications in the future. At the same time, this study provides a reference for guiding perioperative anti-inflammatory therapy. In the future, prospective studies are needed to explore whether anti-inflammatory therapy can bring clinical benefits to patients with gastric cancer.

However, while this study has shown promising results in predicting postoperative complications in patients with gastric

cancer, there are several limitations that need to be addressed. First, the small sample size and the lack of external test data were due to the single-center and retrospective design of the study. Although the model developed using inflammatory indicators and visceral fat demonstrated good efficacy, its generalizability needs to be confirmed through large-scale prospective studies. Furthermore, the exclusion of continuous monitoring of clinical data may limit the accuracy of predictions and long-term clinical outcomes have not been evaluated. Additionally, potential features related to imaging omics markers have not been analyzed, and further investigation into the mechanistic link between visceral fat and gastric cancer is warranted, as this may inform targeted therapeutic interventions. Lastly, the study has not progressed beyond the development stage and requires further refinement to be transformed into a comprehensive system for clinical application, thereby enabling the realization of precision and personalized medicine.

In conclusion, to improve the long-term prognosis of patients undergoing radical gastrectomy, prevention of postoperative complications is crucial. Postoperative complications in patients are typically influenced by factors such as the inflammatory response, nutritional status, and obesity. The integration of clinical-imaging characteristics within the LightGBM model has proven to be effective in predicting the occurrence of postoperative complications in patients with gastric cancer. Therefore, this model is anticipated to serve as a valuable risk assessment tool for postoperative complications of gastric cancer, offering essential insights into the adjustment of surgical strategies and timely postoperative intervention. Ultimately, the LightGBM model has the potential to facilitate early recovery of patients after surgery.

Acknowledgements We would like to appreciate all researchers for their efforts, time, and contributions.

Author Contributions Drs. Chun Yang and Riyue Jiang designed the study and revised the manuscript. Dr. Wenli Wang collected the data, performed the analysis, and drafted the manuscript. The other authors have revised the manuscript accordingly. All authors have approved the final version of the manuscript and the submission.

Funding This study was supported by the Innovative and Entrepreneurial Team of Jiangsu Province grant (JSSCTD202144 (C.Y.)).

Data Availability Data available on request from the authors.

Declarations

Ethics Approval This study was performed in line with the principles of the Declaration of Helsinki. Approval was granted by the Ethics Committee of the First Affiliated Hospital of Nanjing Medical University (22 November 2022/No. 2022-SR-591).

Consent to Participate The requirement for informed consent was waived.

Consent for Publication Not applicable.

Competing Interests The authors declare no competing interests.

References

1. Sung H, Ferlay J, Siegel R L, Laversanne M, Soerjomataram I, Jemal A, Bray F. Global Cancer Statistics 2020: GLOBOCAN Estimates of Incidence and Mortality Worldwide for 36 Cancers in 185 Countries. CA: a Cancer Journal For Clinicians, 2021, 71(3): 209–249
2. H C, Z Z Z, C Z C. [Influence of postoperative complications on prognosis of gastric cancer-The manifestation of gastric surgeon's skill, responsibility and empathy]. Zhonghua wei chang wai ke za zhi = Chinese journal of gastrointestinal surgery, 2023, 26(2)
3. Wu Z, Yan S, Liu Z, Jing C, Liu F, Yu J, Li Z, Zhang J, Zang L, Hao H, Zheng C, Li Y, Fan L, Huang H, Liang P, Wu B, Zhu J, Niu Z, Zhu L, Song W, You J, Wang Q, Li Z, Ji J. Postoperative abdominal complications of gastric and colorectal cancer surgeries in China: a multicentered prospective registry-based cohort study. Science Bulletin, 2022, 67(24): 2517-2521
4. Kanda M, Ito S, Mochizuki Y, Teramoto H, Ishigure K, Murai T, Asada T, Ishiyama A, Matsushita H, Tanaka C, Kobayashi D, Fujiwara M, Murotani K, Kodera Y. Multi-institutional analysis of the prognostic significance of postoperative complications after curative resection for gastric cancer. Cancer Medicine, 2019, 8(11): 5194-5201
5. Shimada H, Fukagawa T, Haga Y, Oba K. Does postoperative morbidity worsen the oncological outcome after radical surgery for gastrointestinal cancers? A systematic review of the literature. Annals of Gastroenterological Surgery, 2017, 1(1): 11-23
6. Xie H, Ruan G, Ge Y, Zhang Q, Zhang H, Lin S, Song M, Zhang X, Liu X, Li X, Zhang K, Yang M, Tang M, Song C-H, Shi H. Inflammatory burden as a prognostic biomarker for cancer. Clinical Nutrition (Edinburgh, Scotland), 2022, 41(6): 1236-1243
7. Bain C R, Myles P S, Corcoran T, Dieleman J M. Postoperative systemic inflammatory dysregulation and corticosteroids: a narrative review. Anaesthesia, 2023, 78(3): 356-370
8. Liu X, Lei S, Wei Q, Wang Y, Liang H, Chen L. Machine Learning-based Correlation Study between Perioperative Immunonutritional Index and Postoperative Anastomotic Leakage in Patients with Gastric Cancer. International Journal of Medical Sciences, 2022, 19(7): 1173-1183
9. Lee D Y, Rhee E-J, Chang Y, Sohn C I, Shin H-C, Ryu S, Lee W-Y. Impact of systemic inflammation on the relationship between insulin resistance and all-cause and cancer-related mortality. Metabolism: Clinical and Experimental, 2018, 81: 52–62
10. Wellen K E, Hotamisligil G S. Obesity-induced inflammatory changes in adipose tissue. The Journal of Clinical Investigation, 2003, 112(12): 1785-1788
11. Shimobayashi M, Albert V, Woelnerhanssen B, Frei I C, Weissenberger D, Meyer-Gerspach A C, Clement N, Moes S, Colombi M, Meier J A, Swierczynska M M, Jenö P, Beglinger C, Peterli R, Hall M N. Insulin resistance causes inflammation in adipose tissue. The Journal of Clinical Investigation, 2018, 128(4): 1538-1550
12. Spyrou N, Avgerinos K I, Mantzoros C S, Dalamaga M. Classic and Novel Adipocytokines at the Intersection of Obesity and Cancer: Diagnostic and Therapeutic Strategies. Current Obesity Reports, 2018, 7(4): 260-275
13. Dalamaga M. Resistin as a biomarker linking obesity and inflammation to cancer: potential clinical perspectives. Biomarkers In Medicine, 2014, 8(1): 107-118
14. Dalamaga M, Diakopoulos K N, Mantzoros C S. The role of adiponectin in cancer: a review of current evidence. Endocrine Reviews, 2012, 33(4): 547-594

15. Lee J W, Son M W, Chung I K, Cho Y S, Lee M-S, Lee S M. Significance of CT attenuation and F-18 fluorodeoxyglucose uptake of visceral adipose tissue for predicting survival in gastric cancer patients after curative surgical resection. Gastric Cancer : Official Journal of the International Gastric Cancer Association and the Japanese Gastric Cancer Association, 2020, 23(2): 273-284
16. Iyengar N M, Gucalp A, Dannenberg A J, Hudis C A. Obesity and Cancer Mechanisms: Tumor Microenvironment and Inflammation. Journal of Clinical Oncology : Official Journal of the American Society of Clinical Oncology, 2016, 34(35): 4270-4276
17. Bian L, Wu D, Chen Y, Ni J, Qu H, Li Z, Chen X. Associations of radiological features of adipose tissues with postoperative complications and overall survival of gastric cancer patients. European Radiology, 2022, 32(12): 8569-8578
18. Li L-M, Feng L-Y, Liu C-C, Huang W-P, Yu Y, Cheng P-Y, Gao J-B. Can visceral fat parameters based on computed tomography be used to predict occult peritoneal metastasis in gastric cancer? World Journal of Gastroenterology, 2023, 29(15): 2310-2321
19. Natsume M, Shimura T, Iwasaki H, Okuda Y, Hayashi K, Takahashi S, Kataoka H. Omental adipocytes promote peritoneal metastasis of gastric cancer through the CXCL2-VEGFA axis. British Journal of Cancer, 2020, 123(3): 459-470
20. Matsui R, Inaki N, Tsuji T, Fukunaga T. Relationship Between Fat Mass Indices and Postoperative Complications After Laparoscopic Gastrectomy in Patients With Gastric Cancer: A Propensity Score Matching Analysis. Anticancer Research, 2022, 42(10): 4841-4848
21. Li L, Li W, Xu D, He H, Yang W, Guo H, Liu X, Ji W, Song C, Xu H, Li W, Shi H, Cui J. Association Between Visceral Fat Area and Cancer Prognosis: A Population-Based Multicenter Prospective Study. The American Journal of Clinical Nutrition, 2023, 118(3): 507-517
22. Takeuchi M, Ishii K, Seki H, Yasui N, Sakata M, Shimada A, Matsumoto H. Excessive visceral fat area as a risk factor for early postoperative complications of total gastrectomy for gastric cancer: a retrospective cohort study. BMC Surgery, 2016, 16(1): 54
23. Wang S-L, Ma L-L, Chen X-Y, Zhou D-L, Li B, Huang D-D, Yu Z, Shen X, Zhuang C-L. Impact of visceral fat on surgical complications and long-term survival of patients with gastric cancer after radical gastrectomy. European Journal of Clinical Nutrition, 2018, 72(3): 436-445
24. Swanson K, Wu E, Zhang A, Alizadeh A A, Zou J. From patterns to patients: Advances in clinical machine learning for cancer diagnosis, prognosis, and treatment. Cell, 2023, 186(8): 1772-1791
25. Lambin P, Leijenaar R T H, Deist T M, Peerlings J, de Jong E E C, van Timmeren J, Sanduleanu S, Larue R T H M, Even A J G, Jochems A, van Wijk Y, Woodruff H, van Soest J, Lustberg T, Roelofs E, van Elmpt W, Dekker A, Mottaghy F M, Wildberger J E, Walsh S. Radiomics: the bridge between medical imaging and personalized medicine. Nature Reviews Clinical Oncology, 2017, 14(12): 749-762
26. Cui Y, Zhang J, Li Z, Wei K, Lei Y, Ren J, Wu L, Shi Z, Meng X, Yang X, Gao X. A CT-based deep learning radiomics nomogram for predicting the response to neoadjuvant chemotherapy in patients with locally advanced gastric cancer: A multicenter cohort study. EClinicalMedicine, 2022, 46: 101348
27. Corey K M, Kashyap S, Lorenzi E, Lagoo-Deenadayalan S A, Heller K, Whalen K, Balu S, Heflin M T, McDonald S R, Swaminathan M, Sendak M. Development and validation of machine learning models to identify high-risk surgical patients using automatically curated electronic health record data (Pythia): A retrospective, single-site study. PLOS Medicine, 2018, 15(11): e1002701
28. Ke X, Cai X, Bian B, Shen Y, Zhou Y, Liu W, Wang X, Shen L, Yang J. Predicting early gastric cancer risk using machine learning: A population-based retrospective study. Digital Health, 2024, 10: 20552076241240905
29. Chen Q, Zhang L, Liu S, You J, Chen L, Jin Z, Zhang S, Zhang B. Radiomics in precision medicine for gastric cancer: opportunities and challenges. European Radiology, 2022, 32(9): 5852-5868
30. Cruz-Bastida J P, Zhang R, Gomez-Cardona D, Hayes J, Li K, Chen G-H. Impact of noise reduction schemes on quantitative accuracy of CT numbers. Medical Physics, 2019, 46(7): 3013-3024
31. C A, K A, H S, Z A, W S B, T F, G D. Noise Reduction in CT Images Using a Selective Mean Filter. Journal of Biomedical Physics & Engineering, 2020, 10(5): 623–634
32. Witten D M, Tibshirani R. Covariance-regularized regression and classification for high-dimensional problems. Journal of the Royal Statistical Society Series B, Statistical Methodology, 2009, 71(3): 615-636
33. Ozenne B, Subtil F, Maucort-Boulch D. The precision--recall curve overcame the optimism of the receiver operating characteristic curve in rare diseases. Journal of Clinical Epidemiology, 2015, 68(8): 855-859
34. Saito T, Rehmsmeier M. The precision-recall plot is more informative than the ROC plot when evaluating binary classifiers on imbalanced datasets. PloS One, 2015, 10(3): e0118432
35. Metz C E. Basic principles of ROC analysis. Seminars In Nuclear Medicine, 1978, 8(4): 283-298
36. Masucci M T, Minopoli M, Del Vecchio S, Carriero M V. The Emerging Role of Neutrophil Extracellular Traps (NETs) in Tumor Progression and Metastasis. Frontiers In Immunology, 2020, 11: 1749
37. Kehlet H. Enhanced postoperative recovery: good from afar, but far from good? Anaesthesia, 2020, 75 Suppl 1: e54-e61
38. Nishijima T F, Muss H B, Shachar S S, Tamura K, Takamatsu Y. Prognostic value of lymphocyte-to-monocyte ratio in patients with solid tumors: A systematic review and meta-analysis. Cancer Treatment Reviews, 2015, 41(10): 971-978
39. Kim C H, Park S M, Kim J J. The Impact of Preoperative Low Body Mass Index on Postoperative Complications and Long-term Survival Outcomes in Gastric Cancer Patients. J Gastric Cancer, 2018, 18(3): 274-286
40. Hsu J-T, Wang C-C, Le P-H, Chen T-H, Kuo C-J, Lin C-J, Chou W-C, Yeh T-S. Lymphocyte-to-monocyte ratios predict gastric cancer surgical outcomes. The Journal of Surgical Research, 2016, 202(2): 284-290
41. Kwak J S, Kim S G, Lee S E, Choi W J, Yoon D S, Choi I S, Moon J I, Sung N S, Kwon S U, Bae I E, Lee S J, Roh S J. The role of postoperative neutrophil-to-lymphocyte ratio as a predictor of postoperative major complications following total gastrectomy for gastric cancer. Annals of Surgical Treatment and Research, 2022, 103(3): 153-159
42. Zhang Z, Weng B, Qiu Y, Feng H, Zhang R, Zhang J, Hu Y, Yu J, Li G, Liu H. Effect of Perioperative Interleukin-6 and Tumor Necrosis Factor-α on Long-Term Outcomes in Locally Advanced Gastric Cancer: Results from the CLASS-01 Trial. Journal of Immunology Research, 2022, 2022: 7863480
43. Chang W-J, Du Y, Zhao X, Ma L-Y, Cao G-W. Inflammation-related factors predicting prognosis of gastric cancer. World Journal of Gastroenterology, 2014, 20(16): 4586-4596
44. Nakauchi M, Vos E L, Tang L H, Gonen M, Janjigian Y Y, Ku G Y, Ilson D H, Maron S B, Yoon S S, Brennan M F, Coit D G, Strong V E. Association of Obesity with Worse Operative and Oncologic Outcomes for Patients Undergoing Gastric Cancer Resection. Annals of Surgical Oncology, 2021, 28(12): 7040-7050
45. Tsekrekos A, Lovece A, Chrysikos D, Ndegwa N, Schizas D, Kumagai K, Rouvelas I. Impact of obesity on the outcomes after gastrectomy for gastric cancer: A meta-analysis. Asian Journal of Surgery, 2022, 45(1): 15-26
46. Pei X, Xie Y, Liu Y, Cai X, Hong L, Yang X, Zhang L, Zhang M, Zheng X, Ning K, Fang M, Tang H. Imaging-based adipose biomarkers for predicting clinical outcomes of cancer patients treated with immune checkpoint inhibitors: a systematic review. Frontiers In Oncology, 2023, 13: 1198723

47. Saravana-Bawan B, Goplen M, Alghamdi M, Khadaroo R G. The Relationship Between Visceral Obesity and Post-operative Complications: A Meta-Analysis. The Journal of Surgical Research, 2021, 267: 71-81
48. Tewari N, Awad S, Macdonald I A, Lobo D N. Obesity-related insulin resistance: implications for the surgical patient. International Journal of Obesity (2005), 2015, 39(11): 1575–1588
49. Okada K, Nishigori T, Obama K, Tsunoda S, Hida K, Hisamori S, Sakai Y. The Incidence of Postoperative Complications after Gastrectomy Increases in Proportion to the Amount of Preoperative Visceral Fat. Journal of Oncology, 2019, 2019: 8404383
50. Shi J, Bao G, Hong J, Wang S, Chen Y, Zhao S, Gao A, Zhang R, Hu J, Yang W, Yan F, Lyu A, Liu R, Cui B, Chen Y, Jin J, Shen B, Zhang Y, Gu W, Feng D, Wang W, Wang J, Wang X, Ning G. Deciphering CT texture features of human visceral fat to evaluate metabolic disorders and surgery-induced weight loss effects. EBioMedicine, 2021, 69: 103471
51. Arai J, Aoki T, Sato M, Niikura R, Suzuki N, Ishibashi R, Tsuji Y, Yamada A, Hirata Y, Ushiku T, Hayakawa Y, Fujishiro M. Machine learning-based personalized prediction of gastric cancer incidence using the endoscopic and histologic findings at the initial endoscopy. Gastrointestinal Endoscopy, 2022, 95(5): 864-872
52. Jiang Y, Liang X, Wang W, Chen C, Yuan Q, Zhang X, Li N, Chen H, Yu J, Xie Y, Xu Y, Zhou Z, Li G, Li R. Noninvasive Prediction of Occult Peritoneal Metastasis in Gastric Cancer Using Deep Learning. JAMA Network Open, 2021, 4(1): e2032269
53. Jiang Y, Zhang Z, Yuan Q, Wang W, Wang H, Li T, Huang W, Xie J, Chen C, Sun Z, Yu J, Xu Y, Poultsides G A, Xing L, Zhou Z, Li G, Li R. Predicting peritoneal recurrence and disease-free survival from CT images in gastric cancer with multitask deep learning: a retrospective study. The Lancet Digital Health, 2022, 4(5): e340-e350